This article was downloaded by: [National Chiao Tung University 國立交通大學]
On: 24 April 2014, At: 22:44
Publisher: Taylor & Francis
Informa Ltd Registered in England and Wales Registered Number: 1072954 Registered office: Mortimer House, 37-41 Mortimer Street, London W1T 3JH, UK

Aerosol Science and Technology
Publication details, including instructions for authors and subscription information:
http://www.tandfonline.com/loi/uast20

Numerical Modeling of Nanoparticle Collection Efficiency of Single-Stage Wire-in-Plate Electrostatic Precipitators

Guan-Yu Lin [a] & Chuen-Jinn Tsai [a]
[a] Institute of Environmental Engineering , National Chiao Tung University , Hsin Chu, Taiwan
Published online: 27 Oct 2010.

To cite this article: Guan-Yu Lin & Chuen-Jinn Tsai (2010) Numerical Modeling of Nanoparticle Collection Efficiency of Single-Stage Wire-in-Plate Electrostatic Precipitators, Aerosol Science and Technology, 44:12, 1122-1130, DOI: 10.1080/02786826.2010.512320

To link to this article: http://dx.doi.org/10.1080/02786826.2010.512320

PLEASE SCROLL DOWN FOR ARTICLE

Taylor & Francis makes every effort to ensure the accuracy of all the information (the "Content") contained in the publications on our platform. However, Taylor & Francis, our agents, and our licensors make no representations or warranties whatsoever as to the accuracy, completeness, or suitability for any purpose of the Content. Any opinions and views expressed in this publication are the opinions and views of the authors, and are not the views of or endorsed by Taylor & Francis. The accuracy of the Content should not be relied upon and should be independently verified with primary sources of information. Taylor and Francis shall not be liable for any losses, actions, claims, proceedings, demands, costs, expenses, damages, and other liabilities whatsoever or howsoever caused arising directly or indirectly in connection with, in relation to or arising out of the use of the Content.

This article may be used for research, teaching, and private study purposes. Any substantial or systematic reproduction, redistribution, reselling, loan, sub-licensing, systematic supply, or distribution in any form to anyone is expressly forbidden. Terms & Conditions of access and use can be found at http://www.tandfonline.com/page/terms-and-conditions

Aerosol Science and Technology, 44:1122–1130, 2010
Copyright © American Association for Aerosol Research
ISSN: 0278-6826 print / 1521-7388 online
DOI: 10.1080/02786826.2010.512320

Numerical Modeling of Nanoparticle Collection Efficiency of Single-Stage Wire-in-Plate Electrostatic Precipitators

Guan-Yu Lin and Chuen-Jinn Tsai
Institute of Environmental Engineering, National Chiao Tung University, Hsin Chu, Taiwan

Downloaded by [National Chiao Tung University] at 22:44 24 April 2014

The numerical models for predicting the collection efficiency of particles in the size range of 0.3 ∼ 10.0 μm in electrostatic precipitators (ESPs) have been well developed. However, for nanoparticles, or particles with the diameter below 100 nm, the existing models can't predict the collection efficiency very well because the electric field and ion concentration distribution were not simulated, or charging models were not adopted appropriately to calculate particle charges. In this study, a 2-D numerical model was developed to predict the nanoparticle collection efficiency in single-stage wire-in-plate ESPs. Laminar flow field was solved by using the Semi-Implicit Method for Pressure-Linked Equation (SIMPLER Method), while electric field strength and ion concentration distribution were solved based on Poisson and diffusion-convection equations, respectively. The charged particle concentration distribution and the particle collection efficiency were then calculated based on the convection-diffusion equation with particle charging calculated by Fuchs diffusion charging theory. The simulated collection efficiencies of 6–100 nm nanoparticles were compared with the experimental data of Huang and Chen (2002) for a wire-in-plate dry ESP (aerosol flow rate: 100 L/min, applied voltage: −15.5 ∼ –21.5 kV). Good agreement was obtained. The simulated particle collection efficiencies were further shown to agree with the experimental data obtained in the study for a wire-in-plate wet ESP (Lin et al. 2010) (aerosol flow rate: 5 L/min, applied voltage: +3.6 ∼ +4.3 kV) using monodisperse NaCl particles of 10 and 50 nm in diameter. It is expected that the present model can be used to facilitate the design of ESPs for nanoparticle control and electrostatic nanoparticle samplers.

INTRODUCTION

Wire-in-plate electrostatic precipitators (ESPs) are widely used to remove suspended particles in the exhaust gas because they are capable of handing large flow rate with low pressure drop through the collection chamber (Oglesby and Nichols 1978). Particles are collected by electrostatic forces, and thus particle electrostatic charge is a very important factor influencing the collection efficiency of the ESPs. Many researchers developed numerical models based on charging models in continuum regime ($Kn = 2\lambda_i/dp \ll \perp$, λ_i: mean free path of ions, d_p: particle diameter) to predict collection efficiency of the wire-in-plate dry ESPs. For particles ranging from 0.3–10 μm in diameter, good agreement between experimental data and numerical results was obtained (Goo and Lee 1997; Park and Kim 2000, 2003; Park and Chun 2002; Talaie 2001, 2005). For particles with $100 \leqq d_p \leqq 200$ nm, the numerical model of Yoo et al. (1997) based on Fuchs diffusion charging model (1947) and the field charging model of Pauthenier and Moreau-Hanot (1932) was able to predict the particle collection efficiency accurately. However, the combined charging model used by Yoo et al. (1997) was found to over-predict particle charge for particles with $d_p \leqq 100$ nm in Lawless (1996), who concluded that 100 nm was the limit of applicability of the combined charging model.

In the transition regime ($Kn \approx 1$), Fuchs model (1963), which was used by Zhuang et al. (2000) and Li and Christofides (2006) to predict particle charge in ESPs, was shown to be accurate for particles with $d_p > 30$ nm (Adachi et al. 1985; Pui et al. 1988). However, the numerical model could not predict the experimental collection efficiency accurately for $30 < d_p < 400$ nm because the flow field and the non-uniform ion concentration distribution were not calculated in Zhuang et al. (2000). In the work of Li and Christofides (2006), non-uniform electric field and ion concentration were not considered either and simulated particle collection efficiencies were not compared with experimental data. Therefore, the applicability of the previous models (Yoo et al. 1997; Zhaung et al. 2000; Li and Christofides 2006) for $30 \leqq d_p \leqq 100$ nm requires further investigation.

For particles with $d_p < 30$ nm, experimental data (Huang and Chen 2002) and numerical results (Yoo et al. 1997; Zhaung et al. 2000; Li and Christofides 2006) showed that a fraction of particles was uncharged and penetrated through the ESPs, resulting in decreasing collection efficiency as d_p was decreased from 30 nm to 5 nm. This is called the partial charging effect. Marlow and Brock's model (1975) was shown to provide accurate prediction of particle charge for $d_p < 30$ nm (Pui et al. 1988). However, Marlow and Brock's model has not

Received 25 May 2010; accepted 24 July 2010.
The financial support of the Taiwan National Science Council through the contract no. NSC 96-2628-E-009-008-MY3 is gratefully acknowledged.
Address correspondence to Chuen-Jinn Tsai, Institute of Environmental Engineering, National Chiao Tung University, No.1001 University Road, Hsin Chu, 300, Taiwan. E-mail: cjtsai@mail.nctu.edu.tw

Downloaded by [National Chiao Tung University] at 22:44 24 April 2014

been applied to examine the partial charging effect on the collection efficiency of the ESP. The combined charging model used in Yoo et al. (1997) over-predicted particle charge in the transition regime, as compared to the experimental data of Fjeld and MacFarland (1986), leading to an overestimation of collection efficiency for particles below 30 nm. The Fuchs model (1963) used in Zhuang et al. (2000) and Li and Christofides (2006) also over-predicted particle charge for $d_p <$ 30 nm, which also led to an overestimation of the collection efficiency.

The present study aims at developing an accurate numerical model to predict nanoparticle collection efficiency in wire-in-plate ESPs using an appropriate particle charging model. The simulated particle collection efficiency will be compared with the experimental data of Huang and Chen (2002) for particles with diameter from 6 to 100 nm. The simulated nanoparticle collection efficiencies will further be validated with the experimental data obtained using monodisperse NaCl particles of 10 and 50 nm in diameter in the wet ESP of Lin et al. (2010).

EXPERIMENTAL METHOD

The schematic diagram of the wet ESP and the experimental setup was described in detailed in Lin et al. (2010). The wet ESP consists of two plexiglass plates on which hydrophilic collection electrodes (100 mm in length, 75 mm in width, and 3.0 mm in thickness) are attached to the inner surface. Between the collection electrodes, a center piece (C) is sandwiched to form a 9 mm gap between the electrodes. On the center piece, three gold discharge wires (GW) (99% purity, 100 μm in diameter, Surepure Chemetals Inc.) spaced at 16 mm in the flow direction are fixed. Test particles used in the experiment were NaCl (particle density = 2200 kg/m^3), which were generated by the evaporation-condensation technique in an oven temperature at temperature of 650–700°C. The generated particles were then passed through a nano-DMA (differential mobility analyzer, TSI Model 3085) to obtain monodisperse particles with d_p of 10 and 50 nm. The experiment was conducted at an aerosol flow rate of 5 L/min and at an applied voltage of $+3.6 \sim +4.3$ kV. A condensation particle counter (CPC, model 3022, TSI Inc.) was used to measure particle number concentration. For 10 and 50 nm particles, the inlet concentration of the ESP was measured to be 1.2×10^9 (m^{-3}) and 6.6×10^9 (m^{-3}), respectively.

The particle collection efficiency of the wet ESP, $\eta_{total}(d_p)$, was calculated as

$$\eta_{total}(d_p)(\%) = \frac{C_{in}(d_p) - C_{out}(d_p)}{C_{in}(d_p)} \times 100\% \qquad [1]$$

where $C_{in}(d_p)$ is the particle inlet concentration (cm^{-3}) and $C_{out}(d_p)$ is the outlet concentration (cm^{-3}) of the ESP for particles with diameter d_p.

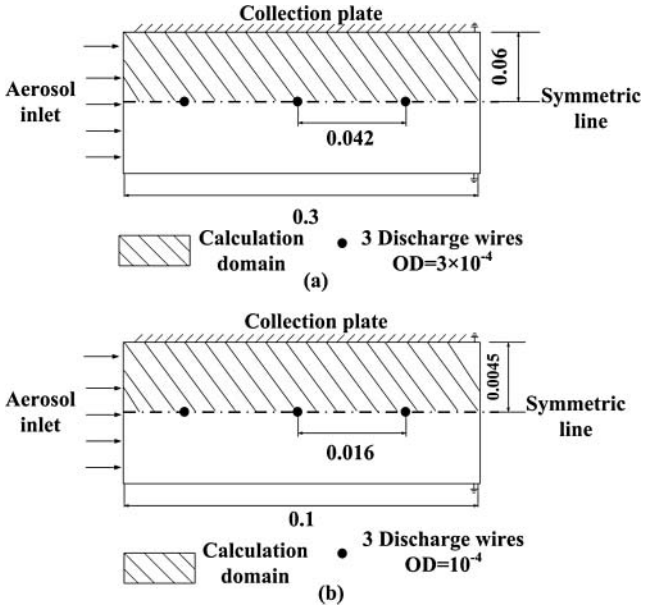

FIG. 1. Calculation domain (a) the single-stage wire-in-plate dry ESP (Huang and Cheng 2002), (b) the single-stage wire-in-plate wet ESP (Lin et al. 2010). (unit: m).

NUMERICAL METHOD

Flow Field

The calculation domains for the dry ESP of Huang and Chen (2002) and the wet ESP (Lin et al. 2010) are shown as the hatched areas in Figures 1a and b, respectively. The dimensions of the present wet ESP (Lin et al. 2010) were described in the previous experimental method section. The wire-in-plate dry ESP in Huang and Chen (2002) was 300 mm in length, 120 mm in width, and 76 mm in height. Three discharge wires had the diameter of 0.3 mm. The wire to wire spacing and wire to plate spacing was 42 and 60 mm, respectively.

A total of 19,368 (269 in x-direction, 72 in y-direction) non-uniform rectangular girds were used in each of the calculation domains. The average grid size was about 62.5 and 372 μm in x and y direction. The smallest size of 2.35 and 1.94 μm was assigned near the wall of the collection plate of the ESP in Huang and Chen (2002) and the present wet ESP, respectively. It was found that increasing the number of girds from 269×72 to 269×92 only resulted in a slight decreasing of particle diffusion loss from 38.5 to 37.6% for 10 nm particles in the present wet ESP. Thus, a fixed number of grid of 269×72 was used in the present simulation. The total number of iterations to reach convergence was about 10,000 for solving the flow field.

The laminar flow field model was used in both cases because the flow Reynolds numbers based on the hydrodynamic diameter were 130.5 and 1124.4 in the wet ESP (Lin et al. 2010) and the dry ESP (Huang and Chen 2002), respectively, which were all smaller than 2000 (Hinds 1999). The governing equations for

the 2-D Navier-Stokes equations are

$$\rho_{air}\left(u\frac{\partial u}{\partial x}+v\frac{\partial u}{\partial y}\right)=-\frac{\partial P}{\partial x}+\mu_{air}\left(\frac{\partial^2 u}{\partial x^2}+\frac{\partial^2 u}{\partial y^2}\right) \quad [2]$$

$$\rho_{air}\left(u\frac{\partial v}{\partial x}+v\frac{\partial v}{\partial y}\right)=-\frac{\partial P}{\partial y}+\mu_{air}\left(\frac{\partial^2 v}{\partial x^2}+\frac{\partial^2 v}{\partial y^2}\right) \quad [3]$$

and the continuity equation is

$$\frac{\partial u}{\partial x}+\frac{\partial v}{\partial y}=0 \quad [4]$$

where u and v (m/s) is the air velocity in x and y direction, respectively, ρ_{air} is the air density (kg/m^3), P is the pressure (Pa), and μ_{air} is the viscosity (kg/m-s). The Navier-Stokes and continuity equations were discretized by means of the finite volume method and solved by the SIMPLER algorithm (Semi-Implicit Method for Pressure-Linked Equations) (Patankar 1980).

Electric Field and Ion Concentration Distribution

The governing equation, Poisson's equation, for the electric field distribution in the ESP can be written as

$$\frac{\partial^2 V}{\partial x^2}+\frac{\partial^2 V}{\partial y^2}=-\frac{\rho_i}{\varepsilon_0} \quad [5]$$

where V is the electric potential (Volt), ρ_i is the space charge density (C/m^3), ε_0 is the permittivity of air (A·sec/V·m).

The space charge density ρ_i in Equation (5) was calculated by the convection-diffusion equation as

$$\frac{\partial(u\rho_i+E_x Z_i\rho_i)}{\partial x}+\frac{\partial(v\rho_i+E_y Z_i\rho_i)}{\partial y}=D_i\left(\frac{\partial^2\rho_i}{\partial x^2}+\frac{\partial^2\rho_i}{\partial y^2}\right) \quad [6]$$

where D_i is the ion diffusion coefficient (m^2/s), Z_i is the ion mobility (m^2/s-V), E_x and E_y are the local electric field strengths at x and y direction (Volt/m), respectively, which can be calculated as

$$-\frac{\partial V}{\partial x}=E_x \quad [7]$$

$$-\frac{\partial V}{\partial y}=E_y \quad [8]$$

Equations (5) and (6) were discretized by using the finite volume method and solved by the same computer code used in the flow field simulation. About 100,000 iterations were needed to reach convergence. In Equation (5), ion quenching by particles was neglected because the predicted ion concentration was much higher than the particle number concentration in this study. For example, when the applied voltage was +3.7 and –15.5 kV, the average ion number concentration was calculated to be 2.26×10^{14} and 1.86×10^{14} (m^{-3}) in the dry and wet ESP, respectively, which was four orders of magnitude higher than the particle concentration. Similarly, in Equation (6), the source term of the corona current generated by charged particles was neglected either. To solve Equations (5) and (6), the ion density at the discharge wire surface must be calculated first as (McDonald et al. 1977)

$$\rho_{i,0}=\frac{2s_x J_p}{\pi Z_i r_c f\left[30\delta+9\left(\frac{\delta}{r_c}\right)^{\frac{1}{2}}\right]}\times10^{-3} \quad [9]$$

where s_x is the half wire to wire spacing (m), r_c is the wire radius (m), f is the wire roughness factor, $\delta=T_0P/TP_0$, T and P are the operational gas temperature (K) and pressure (atm), respectively, $T_0=293$ (K), $P_0=1$ (atm), and J_p is the average current density at the plate (A/m^2) per discharge wire, which is calculated by the analytical equation of Cooperman (1981) as follows:

$$J_p=\frac{\varepsilon_0 Z_i}{16s_y^3}\left(\gamma+\sqrt{\gamma^2+192\left(V_0-V_c\right)\left(s_yE_1\right)}\right) \quad [10]$$

where

$$\gamma=9\left(V_{0.}-V_c+s_yE_1\right)^2-12\left(s_yE_1\right)^2 \quad [11]$$

$$E_1=\frac{\pi V_c}{2s_x\ln\frac{r_{eff}}{r_c}} \quad [12]$$

$$V_c=r_cE_c\ln\frac{r_{eff}}{r_c} \quad [13]$$

$$r_{eff}=\frac{4s_y}{\pi}\text{for}\frac{s_y}{s_x}\le2.0 \quad [14]$$

$$E_c=3\times10^6 f\left(\frac{T_0P}{TP_0}+0.03\sqrt{\frac{T_0P}{TP_0r_c}}\right) \quad [15]$$

In the above equations, s_y is the wire to plate spacing (m), V_0 is the applied voltage (V), V_c is the corona onset voltage (V), E_1 is the average electric field (V/m), r_{eff} is the equivalent cylinder radius (m), and E_c is the corona initiating electric field (V/m).

After obtaining J_p, the total current I (A) per discharge wire is calculated as (McDonald et al. 1977).

$$I=4J_ps_xl \quad [16]$$

where l is the wire length (m).

Downloaded by [National Chiao Tung University] at 22:44 24 April 2014

TABLE 1
Ion molecular weight, ion mobility, and the corresponding ion diffusion coefficient used in previous researches

Z_i (m^2/V-s)		M_i (kg/mol)		D_i (m^2/s)		
Positive ion	Negative ion	Positive ion	Negative ion	Positive ion	Negative ion	Reference
1.40×10^{-4}	1.90×10^{-4}	0.109	0.050	3.6×10^{-6}	4.9×10^{-6}	Adachi et al. (1985)
1.40×10^{-4}	1.90×10^{-4}	0.130	0.100	3.6×10^{-6}	4.9×10^{-6}	Mohnen (1977)
1.40×10^{-4}	1.90×10^{-4}	0.130	0.130	3.6×10^{-6}	4.9×10^{-6}	Wen et al. (1984)
1.40×10^{-4}	1.60×10^{-4}	0.140	0.101	3.6×10^{-6}	4.1×10^{-6}	Wiedensohler and Fissan (1991)
1.35×10^{-4}	1.60×10^{-4}	0.148	0.130	3.5×10^{-6}	4.1×10^{-6}	Wiedensohler et al. (1986)
1.33×10^{-4}	1.84×10^{-4}	0.200	0.100	3.4×10^{-6}	4.7×10^{-6}	Hoppel and Frick (1990)
1.20×10^{-4}	1.35×10^{-4}	0.150	0.090	3.1×10^{-6}	3.5×10^{-6}	Hoppel and Frick (1986)
1.15×10^{-4}	1.39×10^{-4}	0.140	0.101	3.0×10^{-6}	3.6×10^{-6}	Hussin et al. (1983)
1.15×10^{-4}	1.425×10^{-4}	0.290	0.140	3.0×10^{-6}	3.7×10^{-6}	Reischl et al. (1996)
1.15×10^{-4}	1.65×10^{-4}	N.D.	N.D.	3.0×10^{-6}	4.2×10^{-6}	Alonso et al. (2009)

Downloaded by [National Chiao Tung University] at 22:44 24 April 2014

Charged Particles Concentration Distribution and Particle Collection Efficiency

The governing equation of the concentration of particles carrying q elementary charges, $N_{p,q}$, is

$$\frac{\partial(uN_{p,q}+E_xZ_pN_{p,q})}{\partial x}+\frac{\partial(vN_{p,q}+E_yZ_pN_{p,q})}{\partial y} = D_B\left(\frac{\partial^2N_{p,q}}{\partial x^2}+\frac{\partial^2N_{p,q}}{\partial y^2}\right)+S_c+S_p \quad [17]$$

where Z_P is the particle electrical mobility (m^2/s-V), which is defined by $Z_p = qeC_c/3\pi\mu_{air}d_p$, q is the number of elementary units of charge, e is the elementary electrical charge (1.6×10^{-19} C), D_B is the Brownian diffusion coefficient for particles (m^2/s), S_c is the source term, which represents the generation of particles with q elementary charges. In Equation (17), the source term S_c and sink term S_p are given by (Adachi et al. 1985; Aliat et al. 2009)

$$S_c = \alpha_{q-1}N_{p,q-1}N_i \quad [18]$$

$$S_p = -\alpha_qN_{p,q}N_i \quad [19]$$

where α_q is the combination coefficient of positive ions for particles carrying q elementary charges (m^3/s), which is given by (Fuchs 1963)

$$\alpha_q = \frac{\pi\bar{c}_i^+\xi\delta_r^2\exp\left(\frac{-\phi(\delta_r)}{k_bT}\right)}{1+\exp\left(\frac{-\phi(\delta_r)}{k_bT}\right)\frac{\bar{c}_i+\xi\delta_r^2}{4D_ia}\int_0 a/\delta_r\exp\left(\frac{\phi(a/x)}{k_bT}\right)dx} \quad [20]$$

where $\bar{c}_i$ is the mean thermal velocity of ions (m/s), δ_r is the radius of the limiting sphere (m), ξ is the striking probability, k_b is the Boltzmann's constant (J/K), ϕ is the electric potential between the particle and the ion (Adachi et al. 1985) (V), and a is the radius of particles (m). The ξ values shown in Table 1 of Hoppel and Frick (1986) were adopted to investigate the aerosol penetration in the partial charging regime. The parameters used in Equation (20) can be calculated as follows:

$$x = a/r \quad [21]$$

$$\phi(r) = \int_r\infty F(r)dr = \frac{e^2}{4\pi\varepsilon_0}\left[\frac{q}{r}-\frac{\varepsilon_p-1}{\varepsilon_p+1}\frac{a^3}{r^2-a^2}\right] \quad [22]$$

$$\delta_r = \frac{a^3}{\lambda_i^2}\left[\frac{1}{5}\left(1+\frac{\lambda_i}{a}\right)^5-\frac{1}{3}\left(1+\frac{\lambda_i^2}{a^2}\right)\left(1+\frac{\lambda_i}{a}\right)^3+\frac{2}{15}\left(1+\frac{\lambda_i^2}{a^2}\right)^{5/2}\right] \quad [23]$$

$$\xi = \left(\frac{r_a^2\left(1+\frac{2}{3k_bT}(\phi(\delta_r)-\phi(r_a))\right)}{\delta_r}\right)^2 \quad [24]$$

$$D_i = \frac{k_bTZ_i}{e} \quad [25]$$

$$\bar{c}_i = \sqrt{\frac{8k_bT}{\pi(M_i/N_a)}} \quad [26]$$

$$\lambda_i = 1.329\frac{Z_i}{e}\sqrt{\frac{k_bTM_iM_{air}}{(M_i+M_{air})N_a}} \quad [27]$$

where r is the distance between particles and ions center (m), ε_p is the dielectric constant of particles (for NaCl, $\varepsilon_p = 6.12$; for sucrose, $\varepsilon_p = 3.0$), λ_i is the mean free path of ions (m), r_a is the apsoidal distance (m), M_i is the molecular weights of ions (kg/mol), M_{air} is the molecular weights of air (kg/mol), and N_a is the Avogadro number (6.023×10^{23} #/mol). Equation (17) was also discretized by using the finite volume method and solved

Downloaded by [National Chiao Tung University] at 22:44 24 April 2014

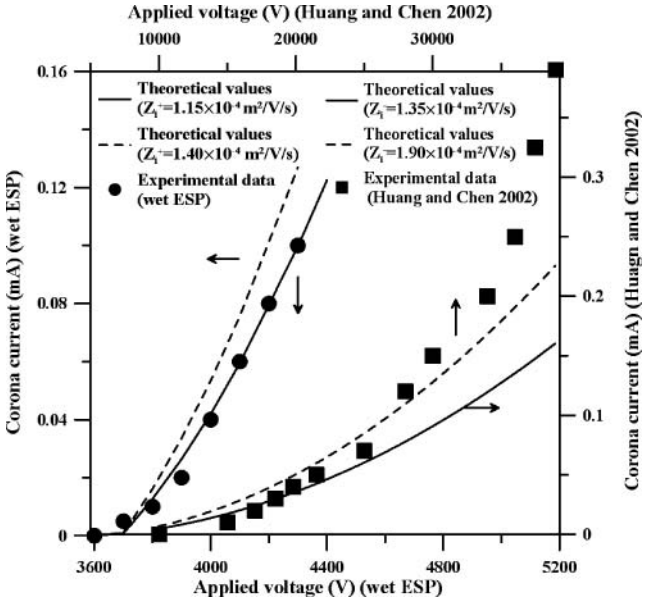

FIG. 2. Comparison of Corona current as a function of applied voltage between theoretical results and experimental data in the ESP.

by the same computer code used in the flow field simulation. About 2000 iterations were needed to reach convergence.

For particles with $d_p \leqq 20$ nm, the charging model of Marlow and Brock (1975) was also applied to examine the partial charging effect on the particle collection efficiency in the present simulation. The combination coefficient α_q was calculated as (Marlow and Brock 1975)

$$\alpha_{q,MB} = \frac{\pi a^2 \bar{c}_i \left[1 + \sqrt{\pi h}\right]}{1 + \left[\lambda_d G_{IN}/1 + \sqrt{\pi h}\right]} \quad [28]$$

where

$$h = \frac{\varepsilon_{p-1}}{\varepsilon_{p+1}} \frac{e^2}{2ak_{bT}} \quad [29]$$

$$\lambda_d = \sqrt{\pi}(a/\lambda_i)\left(\frac{M_i + M_{air}}{M_i}\right) \quad [30]$$

In Equation (28), G_{IN} is the first iterate correction to the flux, which was calculated to be 0.26. After concentrations of particles with different charge levels ($q = 0, 1, 2\ldots$) were obtained, the particle collection efficiency of the ESP was calculated as

$$\eta = \left(1 - \frac{\sum_{q=0}^{n} \int_0^{s_y} N_{p,q,outlet}(y) u_{outlet}(y) dy}{\int_0^{s_y} N_{p,0,inlet}(y) u_{inlet}(y) dy}\right) \times 100\% \quad [31]$$

where $N_{p,0,total}(y)$ is the inlet uncharged particle number concentration, and $N_{p,q,outlet}(y)$ is the outlet number concentration of particles carrying q elementary charges.

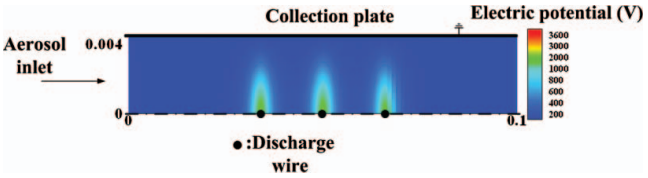

FIG. 3. Electric potential distribution at the applied voltage of +3.7 kV in the wet ESP (Lin et al. 2010). (Note: The scale in y direction is magnified 4.5 times relative to that in x direction.)

RESULTS AND DISCUSSION

Characteristics of the V-I Curve, Electric Field, and Ion Concentration Distribution

Figure 2 shows the comparison of V-I curve between the theoretical values and the experimental data in the dry ESP of Huang and Chen (2002) and the wet ESP (Lin et al. 2010). Applying the ion mobility in the range of $1.35 \times 10^{-4} \sim 1.90 \times 10^{-4}$ m^2/V/s for negative ions and $1.15 \times 10^{-4} \sim 1.40 \times 10^{-4}$ m^2/V/s for positive ions, good agreement was obtained. The range of ion mobility was taken from previous researches and shown in Table 1 (Adachi et al. 1985; Hoppel and Frick 1986; Hussin et al. 1983; Mohnen 1977; Wiedensohler et al. 1986; Wen et al. 1984; Wiedensohler and Fissan 1991). In the mobility range, the variation of the collection efficiency for particles with $2 \leqq d_p \leqq 100$ nm was found to be insignificant, which was calculated to decrease from 3.44 $\sim$ 0.5% to 5.70 $\sim$ 0.0% when the applied voltage was increased from -15.5 to -21.5 kV in the dry ESP of Huang and Chen (2002), and decreased from 3.7 to 0.0% when the applied voltage was increased from +3.6 to +4.3 kV for 10 nm particles in the wet ESP. Thus, a fixed value of 1.35×10^{-4} m^2/V/s for negative ions and 1.15×10^{-4} m^2/V/s for positive ions was used to calculate the particle collection efficiency.

The present simulated electric potential and ion concentration distribution were also compared to the analytical solutions in a wire-in-tube ESP case (Marquard et al. 2005), and numerical results were found to match with analytical solutions (data not shown). Therefore, the present model is able to predict electric field strength and ion concentration distribution in these ESPs. Figures 3 and 4 show the electric potential and the ion density distribution in the wire-in-plate wet ESP (Lin et al. 2010) at an applied voltage of +3.7 kV and an air flow rate was of 5 L/min, respectively. The electric potential is shown to be symmetric

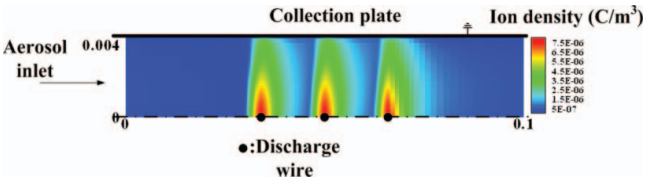

FIG. 4. Ion concentration distribution at the applied voltage of +3.7 kV in the wet ESP (Lin et al. 2010). (Note: The scale in y direction is magnified 4.5 times relative to that in x direction.)

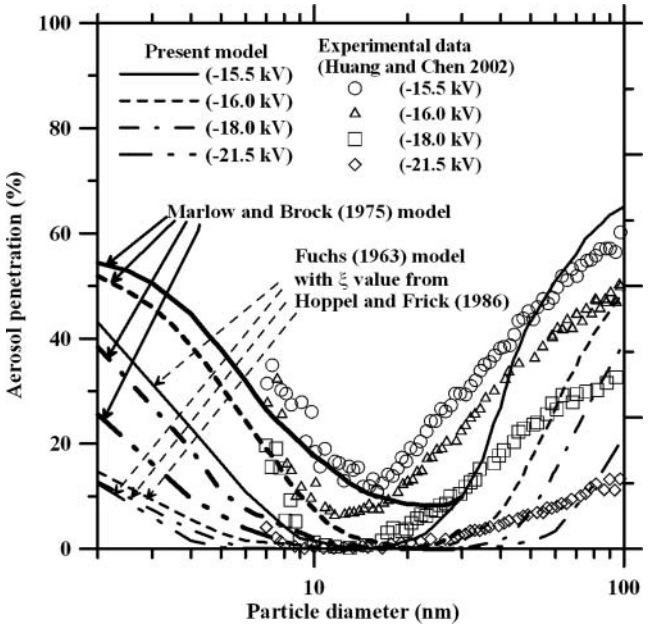

FIG. 5. Comparison of particle collection efficiency in the single-stage wire-in-plage dry ESP between numerical results and experimental data in Huang and Chen (2002) at the aerosol flow rate of 100 L/min.

with respect to the y-axis around the discharge wire. The ion density distribution also tends to be symmetric with respect to the y-axis around the discharge wire. The average ion density at the outlet of the wet ESP, 7.38×10^{-6} C/m^3, was calculated to be slightly higher than 4.69×10^{-7} C/m^3 at the inlet of the wet ESP due to the influence of air flow convection. The profiles of the electric potential and the ion concentration distribution in the dry ESP of Huang and Chen (2002) were found to be similar to those in the wet ESP, and are not shown here.

Comparing the Particle Collection Efficiency in the Dry ESP of Huang and Chen (2002)

Figure 5 shows comparison of the particle collection efficiency between the present numerical values and the experimental data of Huang and Chen (2002). When the aerosol flow rate and the applied voltage was 100 L/min and –15.5 ∼ –21.5 kV, respectively, the numerical results based on Fuchs model (1963) agreed reasonably with experimental data with a deviation of 0.4–11.3% for particles with $40 \leqq d_p \leqq 100$ nm. The calculated penetration efficiencies were 11.3–22.7% lower than the experimental data for particles with $20 \leqq d_p \leqq 40$ nm.

For particles with $d_p \leqq 20$ nm, the present model with particle charge calculated by using Fuchs model (1963) was shown to over-predict the particle collection efficiency with a large deviation of over 20% as compared to the experimental data, as shown in Figure 5. In order to predict the collection efficiency for particles below 20 nm accurately, the charging model of Marlow and Brock (1975) was used in the present simulations. The aerosol penetration was calculated to increase from 0.0 to 38.4% for an applied voltage of –18.0 kV, 0.1 to 51.9% for an applied voltage of –16.0 kV, and 8.52 to 54.4% for an applied voltage of –15.5 kV with decreasing particle diameter from 20 to 2 nm. As shown in Figure 5, better agreement between the simulated values and the experimental data was obtained with deviation of 0.8–13.1% at the applied voltage of –15.5 ∼ –21.5 kV. This result could be attributed to the fact that the model of Marlow and Brock (1975) predicts better combination coefficient than Fuchs model (1963) for particles with $d_p < 20$ nm (Pui et al. 1988; Romay and Pui 1992). The model of Marlow and Brock (1975) considers the velocity distribution of the ions in the vicinity of the particle, which is an important factor for predicting particle charging in the transition and free molecule regimes (Pui et al. 1988). Therefore, it can be concluded that the model of Marlow and Brock (1975) is more appropriate than Fuchs model for predicting particle charging and the collection efficiency in the partial charging regime ($d_p < 20$ nm) in the ESP.

In Figure 5, the ion molecular weight is assumed to be 0.140 kg/mol. The effect of the ion molecular weight on the particle collection efficiency was also examined in the present simulation. Table 1 shows molecular weights of positive and negative ions measured by previous researchers. According to Fuchs theory (1963), the combination coefficient is related to ion molecular weight (Equation (20)). For negative ions, when the ion molecular weight increases from the minimum of 0.05 kg/mol to the maximum of 0.140 kg/mol shown in Table 1, the particle collection efficiency was found to decrease (data not shown) with decreasing α_0 from $3.69 \times 10^{-15} \sim 2.13 \times 10^{-12}$ to $2.85 \times 10^{-15} \sim 1.77 \times 10^{-12}$ for particles with $2 \leqq d_p \leqq 100$ nm. Good agreement between the calculated particle collection efficiency and the experimental data was found to correspond to the ion molecular weight of 0.140 kg/mol. Choosing the minimum ion molecular weight of 0.05 kg/mol leads to a less than 10% deviation between the calculated particle collection efficiencies. For example, when the applied voltage is –15.5 kV, the calculated particle penetration ranges from 12.4 ∼ 17.7% for 10 nm particles, and 40.8 ∼ 43.2% for 50 nm particles, corresponding to the molecular weight range of 0.05–0.14 kg/mol.

To elucidate the aerosol penetration due to the partial charging effect, the concentration distribution of 6 nm particles carrying 0 and 1 charge was calculated at an applied voltage of –15.5 kV and an aerosol flow rate of 100 L/min, as shown in Figure 6. In Figure 6a, high concentration of particles carrying zero charge appears at the outlet of the dry ESP. These uncharged particles can't be collected by electrostatic forces on the collection electrodes, and thus penetrate through the ESP. The average outlet concentration was calculated to be 8.40×10^7 for uncharged particles and 3.54×10^6 m^{-3} for singly charged particle, leading to an average particle charge of 0.04 and an aerosol penetration of 33.0% when the inlet particle concentration was 1.67×10^8 m^{-3}.

When the applied voltage was increased to –21.5 kV, the partial charging effect was less severe than that at the applied voltage of –15.5 kV. It is because the electric field strength and

Downloaded by [National Chiao Tung University] at 22:44 24 April 2014

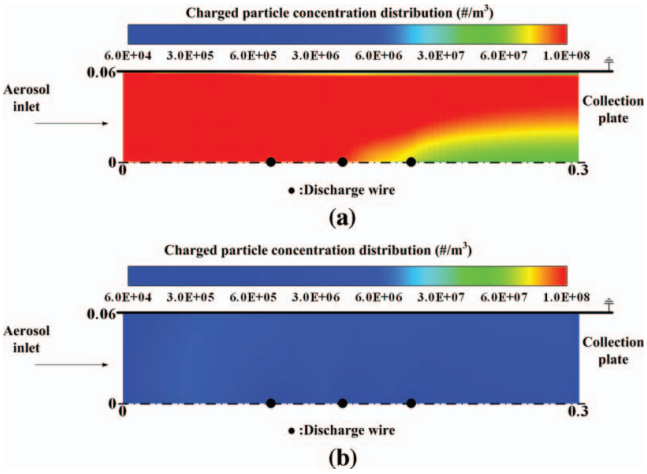

FIG. 6. Number concentration distribution of 6 nm particles carrying 0 and 1 charges in the single-stage wire-in-plate dry ESP (Huang and Chen 2002) when the applied voltage and air flow rate was –15.5 kV and 100 L/min, respectively. (a) 0 charge, (b) 1charge.

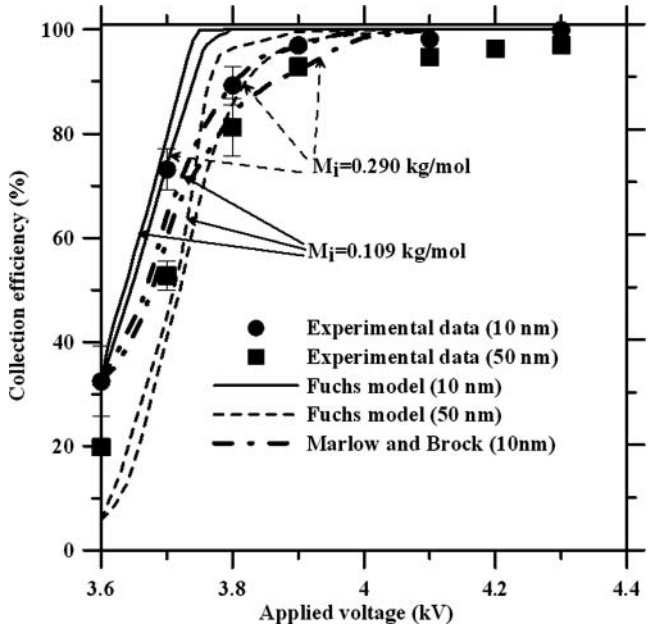

FIG. 7. Comparison of particle collection efficiency in the single-stage wire-in-plage wet ESP (Lin et al. 2010) between numerical results and experimental data at the air flow rate of 5 L/min.

the ion concentration become higher and the particle collection efficiency is enhanced.

For particles with $d_p \geqq 20$ nm at the applied voltage of –15.5 kV, the average particle charge was found to increase from 0.99 to 6.64 with increasing particle diameter from 20 to 100 nm. The partial charging effect on the collection efficiency became insignificant. In this size range, high aerosol penetration was due to weak electric field strength, which can be reduced by applying higher electric filed strength in the ESP.

Comparing the Particle Collection Efficiency in the Present Wet ESP (Lin et al. 2010)

Figure 7 shows comparison of the particle collection efficiency between numerical values and experimental data for 10 and 50 nm NaCl particles in the present single-stage wire-in-plate wet ESP. As the figure shows, when Fuchs model is adopted to calculate the particle charge, the simulated collection efficiencies at the applied voltage of $+3.6 \sim +4.3$ kV agree with the experimental data with deviation of 0.10–10.8% and 4.50–14.1% for 10 and 50 nm particles, respectively. For 10 nm particles, when the model of Marlow and Brock (1975) is used to calculate the particle charge, reasonable agreement between the predicted and the experimental collection efficiency is also obtained with a deviation of 0.10–8.71%.

In Figure 7, the effect of the ion molecular weight on the particle collection efficiency is also shown. Within the range of positive ion molecular weight from 0.109 to 0.290 kg/mol, the corresponding α_0 and α_1 can be calculated based on Fuchs theory as shown in Table 2. The calculated collection efficiency ranges from 74.2 ∼ 79.4% to 100% for 10 nm particles, and from 40.9 ∼ 44.9% to 100% for 50 nm particles, respectively, at the applied voltage of $+3.7 \sim 4.3$ kV. For comparison, the particle collection efficiency ranges from 60.0 ∼ 64.4% to 100% for 10 nm particles at the applied voltage of $+3.7 \sim 4.3$ kV, based on Marlow and Brock's charging model. Again, it shows that there are no significant differences in the particle collection efficiency when different ion molecular weights are used.

Figures 8a–c show the number concentration distribution of 50 nm particles carrying 0, 1, and 4 charges in the wet ESP at an applied voltage of +3.7 kV, an air flow rate of 5 L/min, and an ion molecular weight of 0.290 kg/mol. As shown in the figure, the concentration of particles with 0 charge decreases with increasing x distance from the entrance of the wet ESP, where some particles are charged by positive ions to acquire 1–4 charges and some of which are collected by the collection electrodes due to electrical force. This can be observed from the location of the highest charged particle concentration near the collection electrode surface as shown in Figures 8b and c. Besides, large amount of particles carrying $1 \sim 4$ charges penetrate through the present wet ESP because the electrostatic force is not high enough for collecting the charged particles. The average concentration of particles at the exit of the wet ESP was calculated to be 8.66×10^4, 1.27×10^7, 4.48×10^7, 1.03×10^7, and 2.60×10^5 m^{-3} for particles carrying 0–4 charges, respectively, leading to an average outlet particle charge of 1.97 when the inlet particle concentration was 8.70×10^7 m^{-3}. When the applied voltage was increased to +4.3 kV, the collection efficiency reached up to 99% and the particles carried an average charge of 3.19.

For 10 nm particles, particles with an average outlet concentration of 4.62×10^7 and $2.79 \times 10^6 m^{-3}$ carrying with 0 and 1 charge, respectively, were found to penetrate through the wet ESP operating at +3.7 kV. The average outlet particle charge

Downloaded by [National Chiao Tung University] at 22:44 24 April 2014

TABLE 2
Combination coefficient of positive ion with 50 and 10 nm NaCl particles calculated by using different ion molecular weights shown in Table 1 based on Fuchs theory

$d_p = 50$ nm			$d_p = 10$ nm		
M_{ion} (kg/mol) positive ion	α_0 (m^3/s)	α_1 (m^3/s)	M_{ion} (kg/mol) positive ion	α_0 (m^3/s)	α_1 (m^3/s)
0.109	7.36E-13	1.97E-13	0.109	3.42E-14	1.00E-15
0.130	7.03E-13	1.86E-13	0.130	3.21E-14	9.81E-16
0.140	6.88E-13	1.81E-13	0.140	3.13E-14	9.71E-16
0.148	6.78E-13	1.78E-13	0.148	3.07E-14	9.62E-16
0.150	6.75E-13	1.77E-13	0.150	3.05E-14	9.60E-16
0.200	6.22E-13	1.60E-13	0.200	2.73E-14	9.03E-16
0.290	5.55E-13	1.39E-13	0.290	2.35E-14	8.13E-16

was 0.06, or partial charging occurred which led to a decrease of particle collection efficiency (Figure 7). When the applied voltage was increased to +4.3 kV, the partial charging effect became insignificant, and the collection efficiency of particles with an average charge of 2.00 reached up to 99%.

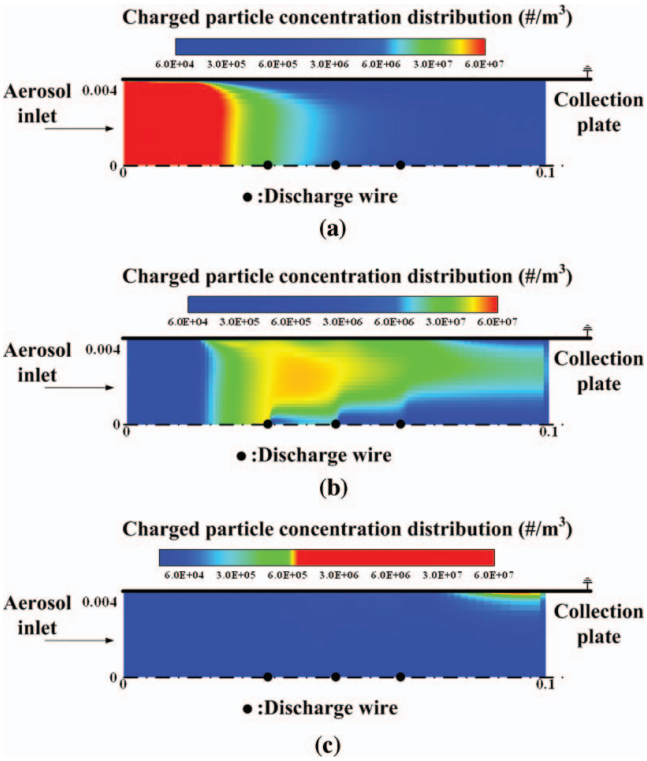

FIG. 8. Number concentration distribution of 50 nm particles carrying 0–4 charges in the single-stage wire-in-plate wet ESP (Lin et al. 2010) when the applied voltage and air flow rate was +3.7 kV and 5 L/min, respectively. (a) 0 charge, (b) 1 charge, (c) 4 charges. (Note: The scale in y direction is magnified 4.5 times relative to that in x direction.)

CONCLUSIONS

This study developed a detailed 2-D mathematical model to predict the flow field, the electric field strength, the ion concentration, the charged particle concentration distribution, and the particle collection efficiency in the single-stage wire-in-plate ESPs. The predicted electric field strength and ion concentration distribution was calculated to match with analytical solutions in a benchmark problem of the wire-in-tube ESP. The comparison of the numerical collection efficiencies based on Fuchs charging model (1963) and the experimental data of the dry ESP in Huang and Chen (2002) shows reasonable agreement with a deviation smaller than 20% for particles with $30 \leqq d_p \leqq 100$ nm. For $d_p < 20$ nm, the predicted aerosol penetration based on the charging model of Marlow and Brock (1975) were found to match better with the experimental data than that based on Fuchs charging model. Aerosol penetration was found to increase with decreasing particle diameter from 20 to 2 nm due to the partial charging effect. In the wet ESP of Lin et al. (2010), the predicted collection efficiencies are also shown to be in good agreement with the experimental data for 50 and 10 nm particles, respectively.

This study shows that partial charging can occur which reduces collection efficiency for particles smaller than 20 nm when the applied voltage is not high enough. Increasing the applied voltage of the ESPs can minimize the partial charging effect and increases the nanoparticle collection efficiency to nearly 100%.

The present numerical model has been validated carefully and can be used to facilitate the design and scale-up of the single-stage wire-in-plate wet ESPs to control the emission of fine and nanosized particles. Furthermore, the present model provides detailed spatial distribution of charged nanoparticles with the consideration of nonuniform distribution of flow field, electric field strength, and ion concentration, which enables the design of efficient electrostatic nanoparticle samplers for sampling and characterization of nanoparticles.

Downloaded by [National Chiao Tung University] at 22:44 24 April 2014

REFERENCES

Adachi, M., Kousaka, Y., and Okuyama, K. (1985). Unipolar and Bipolar Diffusion Charging of Ultrafine Aerosol Particles. *J. Aerosol. Sci.* 16:109–123.

Aliat, A., Hung, C. T., Tsai, C. J., and Wu, J. S. (2009). Implementation of Fuchs Model of Ion Diffusion Charging of Nanoparticles Considering the Electron Contribution in DC-Corona Chargers in High Charge Densities. *J. Phys. D: Appl. Phys.* 42:1–10.

Alonso, M., Santos J. P., Hontañón E., and Ramiro E. (2009). First Differential Mobility Analysis (DMA) Measurements of Air Ions Produced by Radioactive Source and Corona. *Aerosol Air Qual. Res.* 9:453–457.

Cooperman, G. (1981). A New Current-Voltage Relation for Duct Precipitators Valid for Low and High Current Densities. *IEEE Trans. Ind. Appl.* IA-17:236–239.

Fjeld, R. A., and McFarland, A. R. (1986). Continuum Field-Diffusion Theory for Bipolar Charging of Aerosols. *J. Aerosol Sci.* 14:541–556.

Fuchs, N. A. (1947). The Charges on the Particles of Aerocolloids. *Izv. Akad. Nauk. SSSR, Ser. Geogr. Geofiz.* 11:341–348.

Fuchs, N. A. (1963). On the Stationary Charge Distribution on Aerosol Particles in a Bipolar Ionic Atmosphere, *Geophys. Pura. Appl.* 56:185–193.

Goo, J. H., and Lee, J. W. (1997). Stochastic Simulation of Particle Charging and Collection Characteristics for a Wire-Plate Electrostatic Precipitator of Short Length. *J. Aerosol Sci.* 28:875–893.

Hinds, W. C. (1999). *Aerosol Technology*. John Wiley & Sons, New York, p. 30.

Hoppel, W. A., and Frick, G. M. (1986). Ion-Aerosol Attachment Coefficients and the Steady-State Charge-Distribution on Aerosols in a Bipolar Ion Environment. *Aerosol Sci. Technol.* 5:1–21.

Hoppel, W. A., and Frick, G. M. (1990). The Nonequilibrium Character of the Aerosol Charge-Distributions Produced by Neutralizers. *Aerosol Sci. Technol.* 12:471–496.

Huang, S. H., and Chen, C. C. (2002). Ultrafine Aerosol Penetration through Electrostatic Precipitators. *Environ. Sci. Technol.* 36:4625–4632.

Hussin, A., Scheibel, H. G., Becker, K. H., and Porstendoerfer, J. (1983). Bipolar Diffusion Charging of Aerosol-Particles. 1. Experimental Results within the Diameter Range 4-30-nm. *J. Aerosol Sci.* 14:671–677.

Lawless, P. A. (1996). Particle Charging Bounds, Symmetry Relations, and an Analytic Charging Rate Model for the Continuum Regime. *J. Aerosol. Sci.* 27:191–215.

Li, M., and Christofides, P. D. (2006). Collection Efficiency of Nnanosize Particles in a Two-Stage Electrostatic Precipitator. *Ind. Eng. Chem. Res.* 45:8484–8491.

Lin, G. Y., Tsai, C. J., Chen, S. C., Tzu, M. C., and Li, S. N. (2010). An Efficient Single-Stage Wet Electrostatic Precipitator for Fine and Nanosized Particle Control. *Aerosol Sci. Technol.* 44:38–45.

Marlow, W. H., and Brock, J. R. (1975). Unipolar Charging of Small Aerosol Particles. *J. Coll. Interface Sci.* 50:32–38.

Marquard, A., Kasper, M., Meyer, J., and Kasper, G. (2005). Nanoparticle Charging Efficiencies and Related Charging Conditions in a Wire-Tube ESP at DC Energization. *J. Electrostat.* 63:693–698.

McDonald, J. R., Smith, W. B., and Spencer, H. W. (1977). A Mathematical Model for Calculating Electrical Conditions in Wire-Duct Electrostatic Precipitation Devices. *J. Appl. Phys.* 48:2231–2243.

Mohnen, V. A. (1977). *Electrical Processes in Atmospheres*. D. Steinkopff, Darmstadt, pp. 1–17.

Oglesby, S. J., and Nichols, G. B. (1978). *Electrostatic Precipitation*: *Computer model*. Marcel Dekker, Inc., New York, pp. 157–210.

Park, J. H., and Chun, C. H. (2002). An Improved Modelling for Prediction of Grade Efficiency of Electrostatic Precipitators with Negative Corona. *J. Aerosol. Sci.* 33:673–694.

Park, S. J., and Kim, S. S. (2000). Electrohydrodynamic Flow and Particle Transport Mechanism in Electrostatic Precipitators with Cavity Walls. *Aerosol. Sci. Technol.* 33:205–221.

Park, S. J., and Kim, S. S. (2003). Effects of Electrohydrodynamic Flow and Turbulent Diffusion on Collection Efficiency of an Electrostatic Precipitator with Cavity Walls. *Aerosol. Sci. Technol.* 37:574–586.

Patankar, S. V. (1980). *Numerical Heat Transfer and Fluid Flow*. Hemisphere, New York.

Pauthenier, M., and Moreau-Hanot, M. (1932). Charging of Spherical Particles in an Ionizing Field. *J. Phys. Radium* 3:590–613.

Pui D., Y. H., Fruin, S., and McMurry, P. H. (1988). Unipolar Diffusion Charging of Ultrafine Aerosols. *Aerosol Sci. Technol.* 8:173–187.

Reischl, G. P., Mäkelä, J. M., Karch, R., and Necid, J. (1996). Bipolar Charging of Ultrafine Particles in the Size Range Below 10 nm. *J. Aerosol. Sci.* 27:931–949.

Romay, F. J., and Pui, D. Y. H. (1992). On the Combination Coefficient of Positive Ions with Ultrafine Neutral Particles in the Transition and Free-Molecule Regimes. *Aerosol Sci. Technol.* 17:134–147.

Talaie, M. R., Fathikaljahi, J., Taheri, M., and Bahri, P. (2001). Mathematical Modeling of Double-Stage Electrostatic Precipitators Based on a Modified Eulerian Approach. *Aerosol Sci. Technol.* 34:512–519.

Talaie, M. R. (2005). Mathematical Modeling of Wire-Duct Single-Stage Electrostatic Precipitators. *J. Hazard. Mater.* B124:44–582.

Wen, H. Y., Reischl, G. P., and Kasper, G. (1984). Bipolar Diffusion Charging of Fibrous Aerosol-Particles: 1. Charging Theory. *J. Aerosol. Sci.* 15:89–101.

Wiedensohler, A., and Fissan, H. J. (1991). Bipolar Charging-Distributions of Aerosol-Particles in High-Purity Argon and Nitrogen. *Aerosol Sci. Technol.* 14:358–364.

Wiedensohler, A., Lütkenmeier, E., Feldpausch, M., and Helsper, C. (1986). Investigation of the Bipolar Charge-Distribution at Various Gas Conditions. *J. Aerosol. Sci.* 17:413–416.

Yoo, K. H., Lee, J. S., and Oh, M. D. (1997). Charging and Collection of Submicron Particles in Two-Stage Parallel-Plate Electrostatic Precipitators. *Aerosol. Sci. Technol.* 27:308–323.

Zhuang, Y., Kim, Y. J., Lee, T. G., and Biswas, P. (2000). Experimental and Theoretical Studies of Ultra-Fine Particle Behavior in Electrostatic Precipitators. *J. Electrost.* 48:245–260.

Downloaded by [National Chiao Tung University] at 22:44 24 April 2014